Bidirectional Communication Circuits for a 120-GHz PMF Data Link in 40-nm CMOS

Niels Van Thienen, *Student Member, IEEE*, Yang Zhang, *Student Member, IEEE*, and Patrick Reynaert, *Senior Member, IEEE*

***Abstract*— Three different bidirectional polymer microwave fiber (PMF) links are presented and discussed. The proposed solutions exploit the following orthogonal signaling dimensions: wave direction, wave polarity, and signal polarity. First, a 120-GHz substrate integrated waveguide directional coupler is implemented and exploits the wave direction orthogonality. The 4-port on-board hybrid coupler achieves measured data rates of, respectively, 6 and 5.5 Gbps in the up- and down-link over a distance of 8 m. Second, a 120-GHz ortho-mode transducer (OMT) is micro-machined and exploits the wave polarity orthogonality. The micro-machined polarization duplexer has a measured isolation of 45 dB over the entire *F*-band. For the horizontal and vertical paths, the insertion loss is measured with a 40-cm-long Teflon fiber and varies between −5 and −9 dB. Finally, a 120-GHz in-band full-duplex (IBFD) PMF transceiver with tunable electrical-balance duplexer (EBD) and on-chip bow-tie antenna are implemented in a 40-nm bulk CMOS technology. In this case, the duplexing principle is relying on signal polarity. The self-interference (SI) cancellation is achieved with a fully differential transformer-based EBD, resulting in a simulated SI suppression of 30 dB over a bandwidth of more than 14 GHz. The insertion loss of the duplexer is less than 11 dB from TX to fiber and less than 12 dB from fiber to RX at a frequency of 120 GHz. The balancing network provides an impedance locking range from 45 to 93 Ω and 38 to 266 fF at 120 GHz. For IBFD operation, the maximum measured data rate is 6.2 Gbps. The transceiver with integrated antenna occupies an area of 1.8 mm x 1.53 mm and has a dc power consumption of 73 mW in total.**

***Index Terms*— 120 GHz, CMOS, electrical-balance duplexer (EBD), in-band full-duplex (IBFD), millimeter-wave, ortho-mode transducer (OMT), polymer microwave fiber (PMF), self-interference (SI) cancellation, substrate-integrated waveguide (SIW) directional coupler, tunable balancing network.**

I. Introduction

IN RECENT years, research on polymer microwave fiber (PMF) communication links in bulk CMOS [1]–[4] has been increasingly popular. State-of-the-art simplex PMF communication links enable data rates up to 18 Gbps and allow transmitting distances up to 15 m [3]. Only few papers have investigated the possibilities to create a bidirectional PMF link [4], [5]. The self-interference (SI) phenomenon—the problem of signal leakage from the transmitter into its own receiver—has to be addressed in several stages of the communication chain. For example, suppression of the SI signal can be done at the antenna interface in the RF domain. In a next step, the residual SI can be compensated in the analog part of the receiver. The remainder of the SI product that has not been completely canceled out, can be compensated by digital cancellation in the final stage of the receiver chain.

In Section II, an overview of bidirectional communication techniques will be given with a strong focus on the suitability for millimeter-wave and PMF applications. A theoretical explanation of the listed duplex techniques will be given. Results of several implemented concepts will be discussed and analyzed, and the measurement results will be shown. Goldsmith [6] stated: "bidirectional systems must separate the up- and down-link channels into orthogonal signaling dimensions," which means that a bidirectional link has to behave orthogonally between up- and down-link. This is needed in order to reduce SI and to avoid that both up- and down-link signals become indistinguishable. The concept of orthogonality is successfully implemented at frequencies above 100 GHz. These duplex techniques exploit an orthogonal behavior in one of the following dimensions: wave polarity (Section II-B), wave direction (Section II-A), and signal polarity (Section II-C).

II. Bidirectional Communication Techniques

The ultimate goal is an *in-band full-duplex* (IBFD) system where the SI signals are canceled. This can be obtained in several ways. SI occurs when one transmits and receives simultaneously at the same frequency. This results in an overpowered received signal with the unwanted transmitted signal. Cancellation can be done in the analog or digital domain. In fact, the transmitter knows exactly what has been sent. To cancel the SI, a modified copy of the transmitted signal needs to be subtracted from the received signal. The residual analog part that has not been canceled out completely can be compensated by digital cancellation. As stated in [7], the most promising techniques are passive cancellation, active analog cancellation, active digital cancellation, and passive suppression. IBFD might also an interesting concept for wireless communication according to [8].

In the following paragraphs, three different duplex concepts will be discussed that use orthogonal dimensions different from time, frequency, or space. The main motivation to investigate the bidirectional operation for PMF links that does not compromise time, frequency, or space is the need for a

Manuscript received November 29, 2017; revised February 15, 2018 and March 22, 2018; accepted March 23, 2018. Date of publication April 19, 2018; date of current version June 25, 2018. This paper was approved by Guest Editor Andrea Bevilacqua. *(Corresponding author: Yang Zhang.)*

The authors are with the Department of Electrical Engineering, Micro-Electronics and Sensors, University of Louvain, B-3001 Louvain, Belgium (e-mail: yang.zhang@esat.kuleuven.be).

Color versions of one or more of the figures in this paper are available online at http://ieeexplore.ieee.org.

Digital Object Identifier 10.1109/JSSC.2018.2822714

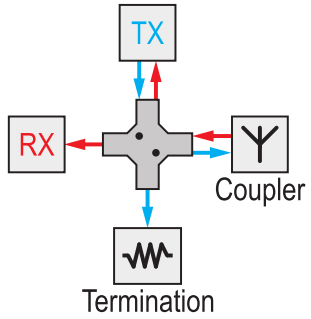

Fig. 1. Working principle of a directional coupler. An incoming signal propagates to only two of the three remaining ports.

single-channel bidirectional link that operates simultaneously at the same frequency. The IBFD techniques discussed in this paper exploit orthogonal signaling dimensions, in particular, the wave direction, the wave polarity, and the orthogonality between common and differential mode are discussed.

A. Propagation Direction

Directional couplers are 4-port passive building blocks where one port is isolated from the input port, as illustrated in Fig. 1. As a result, the incoming signal propagates to only two of the three remaining ports. Because the power is then split in two different directions—and thus divided over two ports—only half of the signal arrives at the receiver port. This is also true for the transmit side, resulting in a total loss of $3 + 3$ dB for a link with two directional couplers. The directional coupler has a reciprocal behavior that allows its usage in bidirectional communication systems. In the presented SIW directional coupler design, a Megtron6 substrate is used. The measurement results are reported in Section III. Three severe issues were encountered during the measurements: 1) printed circuit board (PCB) manufacturability and accuracy are insufficient; 2) no tuning options are available to change the impedance; and 3) internal reflections in the SIW due to mismatch at the PCB interface kill the isolation between TX and RX, sacrificing the performance.

B. Propagation Polarity

Polarization division duplex has already been demonstrated with a PMF link in [9] and [10]. The orthogonality between a horizontal and vertical polarization distinguishes the up- and down-link. This technique is commonly used in satellite communication, where up- and down-link have an orthogonal circular polarization. As a result, it can provide relative high isolation values between the up- and down-link signals. One of the major drawbacks of polarization duplex is the more complex antenna structure needed to launch waves with orthogonal polarizations. Those polarizations can be, for example, circular or horizontal and vertical. A 120-GHz implementation using an ortho-mode transducer (OMT) is proposed in this paper. The measurement results are reported in Section IV. For linear polarization, the transmitter and receiver need to be aligned with each other, to make sure the antennas receive the polarized signal with maximum signal strength. This is not the case for circular polarization, where the polarization

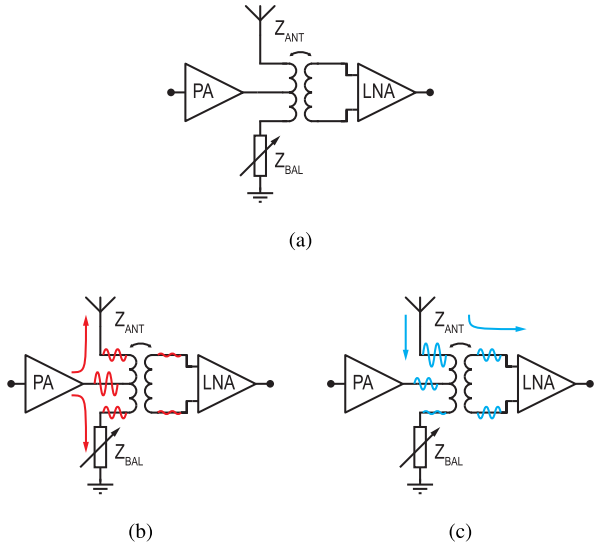

Fig. 2. Working principle of (a) EBD in (b) transmitting and (c) receiving mode.

is insensitive for the absolute aligning of the transmitter and the receiver. A drawback of circular polarized waves is that they can become elliptical polarized due to disturbances, bends, or other imperfections in the channel. Reflections of the direct wave are a major concern. They can occur at the interface between the fiber and the antenna at transmitter and receiver side.

C. Signal Polarity

The EBD design overcomes the issues that are encountered in the SIW directional coupler: 1) the accuracy is now increased because the duplexer is fully integrated on chip level; 2) tuning is made possible by adding a balancing network; and 3) the reflections in the SIW are avoided. A considerable amount of the literature has been published on the design of EBD [11]–[18] in the sub-millimeter-wave frequency range. Recently, EBD designs operating in the millimeter-wave frequency range have been published [19], [20]. Fig. 2(a) shows the schematic of an EBD. Fig. 2(b) and (c) illustrates the working principle of the hybrid transformer in TX and RX mode, respectively. The EBD concept is based on balancing the impedances observed at the antenna and the balancing network of the hybrid transformer. If both impedances match properly, no current is induced in the secondary transformer winding for TX operation. In RX operation, the transformer transfers half of the power to the receiver. Impedance tuning becomes especially sensitive at millimeter-wave frequencies. The EBD design has a theoretical loss of 3 dB for both the transmit and receive path, similar to the SIW directional coupler. This results in a total loss of $3 + 3$ dB for a PMF communication link with two EBD duplexers. A more profound analysis is given in Section V.

III. 120-GHz Substrate Integrated Waveguide Directional Coupler Design

To enable duplex operation without increasing the bandwidth, an in-band duplexer was realized using a substrate

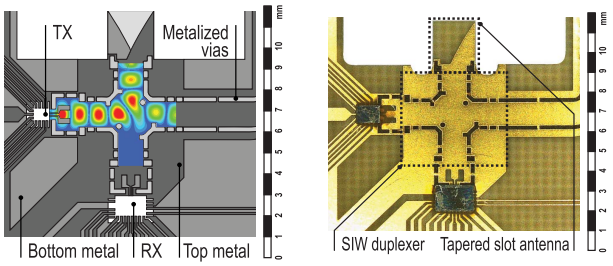

Fig. 3. Top view of (a) SIW directional coupler model and (b) flip-chip bonded implementation on a Megtron6 substrate.

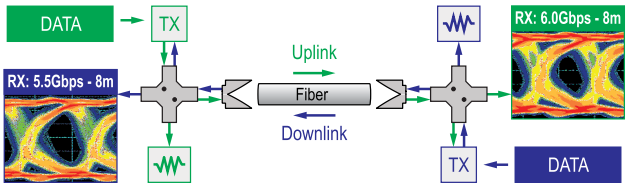

Fig. 4. Half-duplex measurement setup for the up- and down-link over 8 m of Teflon fiber at a maximum data rate of 5.5 Gbps.

integrated waveguide (SIW) directional coupler [2] at 120 GHz. It makes use of the orthogonality between propagation directions to reduce the SI signal. A time-interleaved solution, using a 4-port on-board hybrid coupler, is shown in Fig. 3. Isolation between the transmitter and receiver is realized with several metalized vias within the SIW, as shown in Fig. 3. The transmitter and receiver chip share the same antenna.

The measurement setup of the duplex communication is described in Fig. 4. An 8-m-long hollow Teflon fiber connects both transceivers. Two oscilloscopes validate the bit error rate (BER) of the half-duplex link. Data rates of, respectively, 6 and 5.5 Gbps were measured separately in the up- and down-link over a distance of 8 m. The asymmetry in data rate is due to a mismatch between the TX and RX duplexers, mainly caused by the flip-chip placement and tolerances on the fabricated Megtron6 substrate. Although the hybrid coupler would enable IBFD operation, the near-end crosstalk caused by reflections at the coupler-fiber interface limits the ultimate TX-RX isolation that can be achieved from this solution. The entire duplex solution—including the antenna, the duplexer, and the TX and the RX chips—consumes a board area of less than 1 cm^2.

IV. 120-GHz Ortho-Mode Transducer Design

Another approach to maintain IBFD is polarization duplex. Initial research indicates that polarization orthogonality is maintained in the fiber, even when bending the fiber. In a rectangular shaped fiber, the polarization stays aligned according to the rotation of the fiber. Compared with a circular fiber, the polarization is uncorrelated with the fibers geometry, since the shape is point symmetrical. In that case, the TX and RX antennas have to be aligned. The polarization of both OMT transceivers has to be aligned with each other.

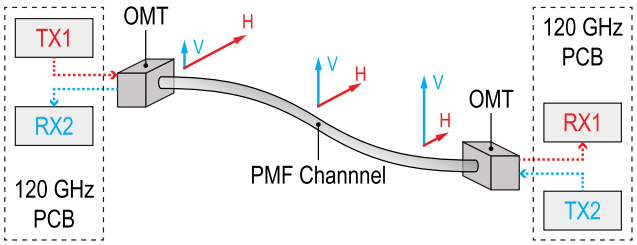

Fig. 5. System of a bidirectional link using two orthogonal linear polarizations. The vertical and horizontal modes are separated using an OMT.

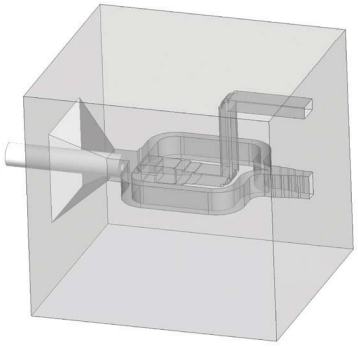

Fig. 6. 3-D model of the OMT design with a PMF port at the left side and two orthogonal linearly polarized ports at the right side.

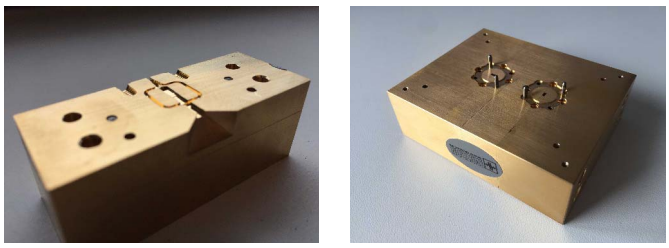

(a) (b)

Fig. 7. Picture of a (a) single fabricated part of the OMT and (b) entirely assembled OMT block existing of four parts.

The proposed bidirectional setup with the 120-GHz OMT, also known as a polarization duplexer, is illustrated in Fig. 5. The study of various OMT types have been well performed by [21]–[23]. In this design, we optimized the OMT—which is based on the Boifot type [21]—for maximal isolation between TX and RX. The OMT implementation is shown in Fig. 6. The OMT block has three external ports: one port to insert the Teflon waveguide at the left and two orthogonal linearly polarized WR-8 metal waveguide ports at the right. The OMT block is micro-machined. State-of-the-art milling techniques are used to achieve mechanical tolerances below 10 μm. The entire OMT block is divided in three sub-blocks for manufacturability reasons. A picture of one single block and the assembled OMT block are depicted in Fig. 7(a) and (b), respectively.

As can be seen in Fig. 8, the average isolation is 45 dB over the entire F-band. For the horizontal and vertical paths, the insertion loss is measured with a 40-cm-long Teflon fiber and varies between -5 and -9 dB, including the losses in the OMT.

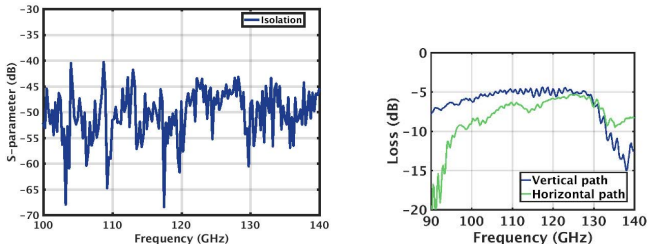

(a) (b)

Fig. 8. Measured (a) isolation and (b) insertion loss for horizontal and vertical mode OMT operation.

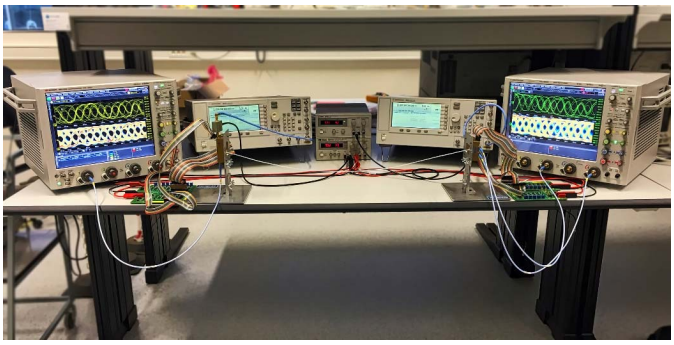

Fig. 9. Bidirectional operation is demonstrated using polarization division duplex. This allows to transmit and receive simultaneously sharing the same coupler, fiber, and frequency.

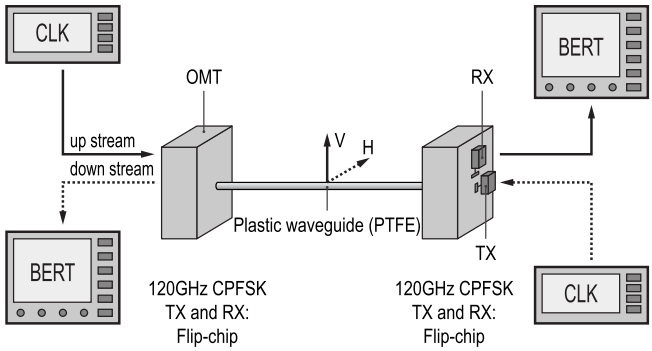

Fig. 10. OMT measurement setup over 1 m of Teflon fiber at a maximum data rate of $10 + 10$ Gbps.

The system setup is shown in Fig. 9. Up- and down-link travel together through one single circular Teflon fiber with an outer diameter of 2 mm. Two orthogonal linear polarized modes are launched in the fiber. Two OMTs, both including transmitter and receiver, are placed in front of each other and are connected using a Teflon fiber. Two Keysight E8257D PSG signal generators trigger the on-chip pseudorandom binary sequence (PRBS) inputs of both up- and down-link transmitters. At the receiver side, a Keysight DSAZ634A 63-GHz oscilloscope and an Agilent DSOX92004A Infiniium 20-GHz oscilloscope show the demodulated differential output signal of both receivers without any error correction or equalization. The eye diagrams are clearly visible on the oscilloscopes.

The entire link is measured with a 1-m-long PMF channel as illustrated in Fig. 10. Two different PRBS data sequences

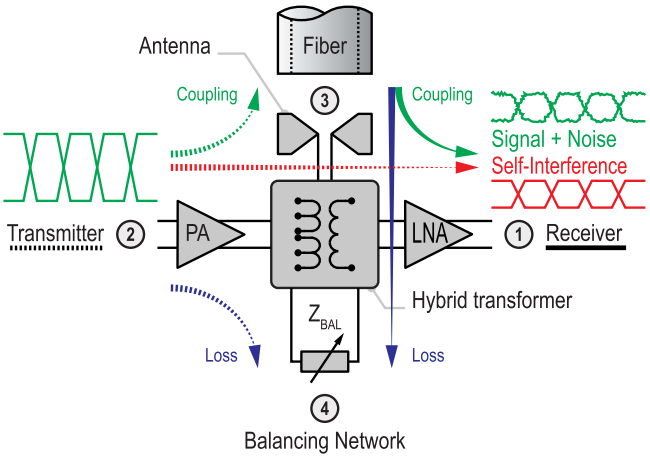

Fig. 11. Architecture of the proposed transformer-based duplexer. The hybrid transformer is the core of the system and realizes the isolation between PA and LNA to suppress the SI signal.

are used in the parBERT to distinguish up- and down-link. The proposed in-band duplex link supports a simultaneous $10 + 10$ Gbps data rate through one single channel with a BER less than 10^{-12}.

V. 120-GHz Electrical-Balance Duplexer Design in 40-nm CMOS

In this section, the design of an integrated IBFD transceiver will be presented, where transmitter and receiver simultaneously use the same frequency band while communicating through the same channel. IBFD is superior compared to traditional techniques such as half and full duplex in terms of data throughput. The aim of this section is to design and implement an EBD transceiver at millimeter-wave frequencies for a PMF communication link, with a measured link as result. A 120-GHz IBFD PMF transceiver with tunable EBD with on-chip antenna is implemented in a 40-nm bulk CMOS technology. The SI cancellation is performed with a fully differential transformer-based EBD, resulting in a simulated SI suppression of 30 dB over a bandwidth of more than 14 GHz. The insertion loss of the duplexer is less than 11 dB from TX to fiber and less than 12 dB from fiber to RX at a frequency of 120 GHz. The balancing network impedance can tolerate load impedances from 45 to 93 Ω and 38 to 266 fF at 120 GHz. For IBFD operation, the maximum measured data rate is 6.2 Gbps. The transceiver with integrated antenna occupies an area of 1.8×1.53 mm^2 and has a dc power consumption of 73 mW in total.

A. IBFD Transceiver Architecture

The EBD design [24] is based on balancing the impedances observed at the antenna and the balancing network of the hybrid transformer as illustrated in Fig. 11. This results in a suppressed signal transfer from transmitter to receiver, enabling bidirectional operation. A drawback of the EBD technique is the 3-dB inherent loss in both transmitter and receiver paths, resulting in $3 + 3$ dB insertion loss for the entire link budget. The proposed 120-GHz IBFD transceiver

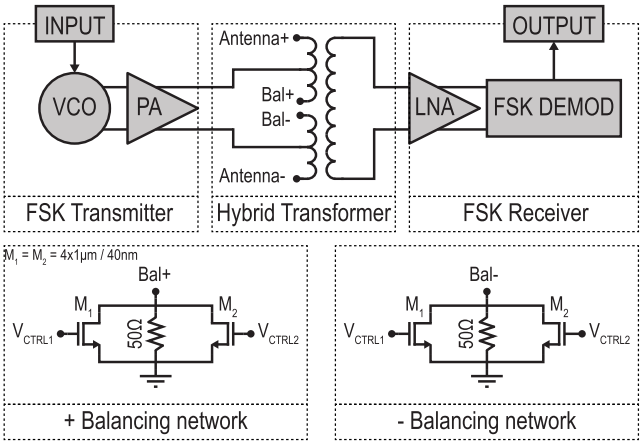

Fig. 12. Schematic of a fully differential transformer-based EBD. The on-chip antenna and the on-chip balancing network form the major building blocks of the implemented transceiver.

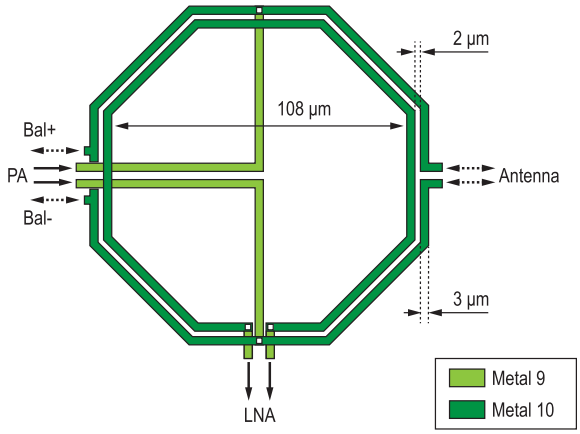

Fig. 13. Detailed layout of the hybrid transformer. The inner and outer windings are designed in metal 10 while the interconnect to the PA is constructed in metal 9.

is implemented as a fully differential transformer-based EBD as illustrated in Fig. 12. The hybrid transformer is the key building block and connects transmitter and receiver to the antenna in such a way that: 1) the isolation between power amplifier (PA) and LNA is sufficiently high to reduce the SI leakage and 2) the insertion loss from PA to fiber (S_{32}) or fiber to LNA (S_{13}) stays as low as possible.

To achieve high data rates, the major challenge is to design the EBD with sufficient broadband isolation in the millimeter-wave frequency range. This can only be attained when the balancing network impedance matches the antenna impedance closely over the desired bandwidth. The exact impedance observed at the antenna feed depends on the composition of the entire coupling structure, including fiber and on-chip antenna. High isolation is, therefore, hard to achieve at millimeter-wave frequencies, especially in combination with low insertion losses. The hybrid transformer duplexer is designed in combination with an on-chip bow-tie antenna. A bow-tie antenna has a broadband behavior, and therefore, facilitates the design of the balancing network. The entire duplexer including coupler is designed for a minimum isolation of 30 dB and maximum insertion loss of only 12 dB over a 10-GHz bandwidth.

B. Transmitter and Receiver Circuitry

The transmitter generates a two-tone continuous phase frequency-shift keying (CPFSK) signal with 4-GHz tone spacing at a carrier frequency of 120 GHz and an RF power of -1.9 dBm. The receiver demodulates the signal and drives a 50-Ω load. At 6.2 Gbps, the transmitter and receiver have a dc power consumption of 13.56 and 59.41 mW, respectively, with a supply voltage of 0.9 V. A more detailed study on the transmitter and receiver circuitry can be found in [1].

C. Hybrid Transformer

The layout of the hybrid transformer at 120 GHz is depicted in Fig. 13. The transformer is designed in the two topmost metal layers to minimize the resistive losses. The outer diameter is 124 μm and the traces are 3 μm wide. A fully differential topology was chosen to facilitate the interconnect with the four surrounding circuits. A transformer-based matching network is used for impedance matching and allows to perform biasing for the PA and LNA.

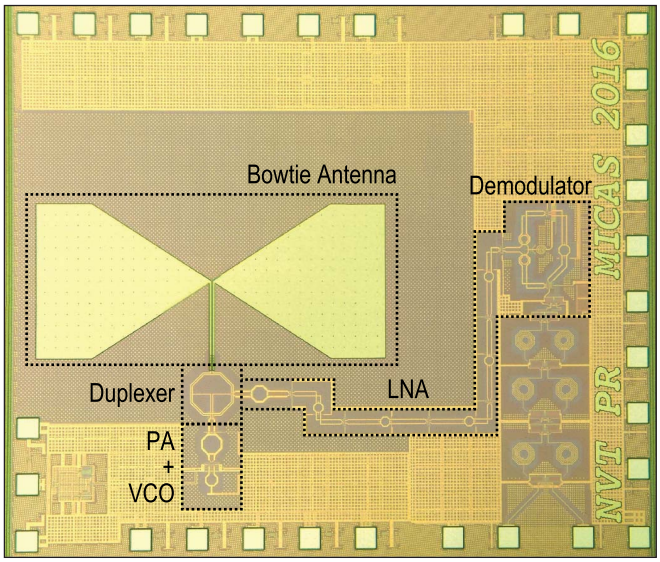

Fig. 14. Die micrograph of the transceiver chip with outer dimensions of 1.8×1.53 mm^2. The bow-tie dipole antenna occupies an area of 0.44×1 mm^2 and is fabricated in the aluminum top metal.

D. Broadband Coupler

A bow-tie antenna couples to the fundamental HE_{11} mode in the polymer fiber. The broadband behavior of such antenna relaxes the specifications of the balancing network. The antenna is fabricated in the aluminum top metal as illustrated in Fig. 14. The antenna implementation is depicted in Fig. 15. To improve the coupling efficiency, a metal cage reflector is placed at the bottom of the Megtron6 PCB that reflects the electromagnetic (EM) wave back into the fiber as shown in Fig. 16. The metal cage is constructed in a three-layer PCB as highlighted in Fig. 17. Metalized buried vias form the side walls to avoid that the EM waves radiate in

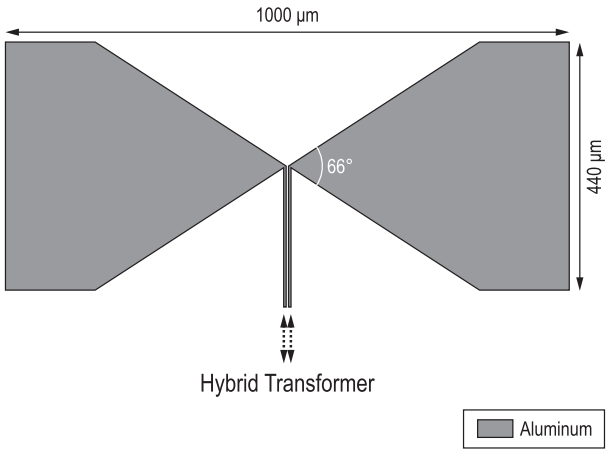

Fig. 15. Broadband antenna implemented as bow-tie dipole with an impedance of 52-j17 Ω at 120 GHz. The antenna size is 440 μm × 1000 μm.

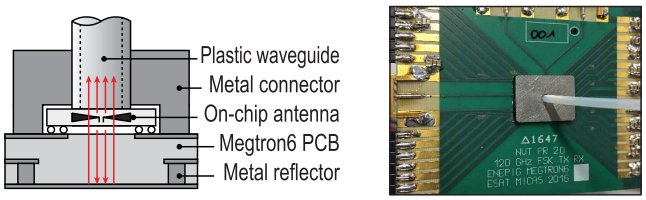

Fig. 16. Coupler implementation [1] including a 2-mm hollow PTFE fiber, a three-layer Megtron6 PCB, a metal connector, and a metal cage reflector. At 120 GHz, the entire coupler has a simulated loss of 7.1 dB.

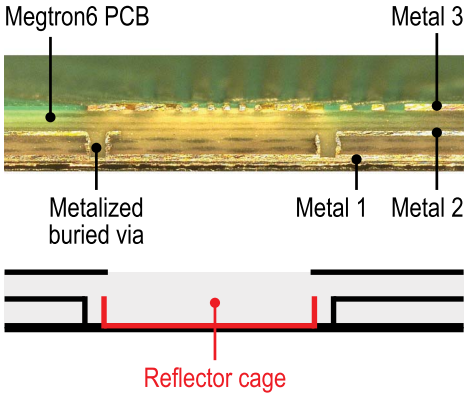

Fig. 17. Cross section of the three-layer PCB. The bottom layer acts, in combination with the metalized buried vias, as a metal reflector cage to minimize the radiation losses into the Megtron6 substrate.

the PCB substrate. The entire coupling structure from antenna feed to fiber is simulated in HFSS and has an insertion loss of 7.1 dB with an impedance of 52-j17 Ω at 120 GHz. The antenna measures 0.4 × 1 mm and the hybrid transformer has an outer diameter of 124 μm.

E. Balancing Network

To match the impedance of the broadband dipole antenna, the balancing network consists of a p+ poly resistor of 50 Ω and two nMOS transistors as illustrated in Fig. 12 and can be controlled using V_{ctrl1} and V_{ctrl2}. As a result, the balancing

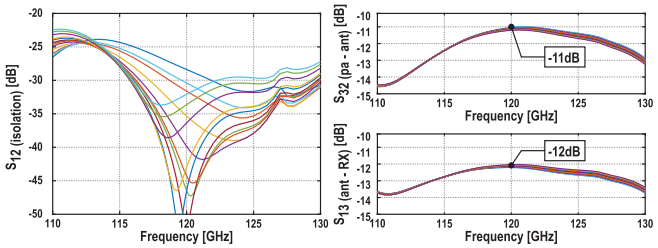

Fig. 18. Simulated S-parameters of the entire EBD including coupler and fiber. S_{32} and S_{13} have, respectively, 11 and 12 dB insertion loss, while the isolation S_{12} can be tuned over frequency.

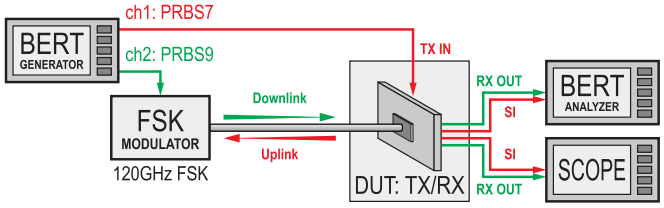

Fig. 19. IBFD measurement setup. A BERT generates a PRBS9 pattern for the down-link and a PRBS7 pattern for the up-link to distinguish the SI from the signal in the analyzer. An oscilloscope captures the eye diagram.

network impedance can tolerate load impedances between 92 − j34 Ω and 45 − j5 Ω corresponding to a resistance between 45 and 93 Ω and a capacitance between 38 and 266 fF at 120 GHz. Fig. 18 shows the simulation results of the isolation capability for different tuning settings. This results in a simulated SI suppression of 30 dB over a bandwidth of more than 14 GHz. The duplexer insertion loss is less than 11 dB from TX to fiber and less than 12 dB from fiber to RX at a frequency of 120 GHz and is nearly independent for the different settings of the balancing network. The insertion loss suffers mainly from the increased substrate loss at millimeter-wave frequencies and mismatch at the antenna coupling due to a limited quality factor of the passive components.

F. Measurement Results

The presented chip, of which a die micrograph is shown in Fig. 14, is implemented in a 40-nm bulk CMOS technology. The transmitter and receiver occupy an active area of 0.025 and 0.43 mm^2, respectively.

The IBFD measurement setup is shown in Fig. 19. To measure the isolation, a 120-GHz two-tone CPFSK modulator launches a PRBS9 pattern with a power level of −6 dBm in the fiber toward the transceiver, which receives and demodulates that signal while simultaneously transmitting a PRBS7 pattern. A Keysight 81250 parBERT verifies the demodulated PRBS9 signal, resulting in a maximum measured data rate of 6.2 Gbps with a BER below 10^{-12}. The eye diagrams, captured with a Keysight DSO-Z 634A 63-GHz 160-Gs oscilloscope, are presented in Figs. 20 and 21 for different bias settings of the balancing network. Fig. 20 illustrates the effect of tuning the balancing network on the SI signal. If only the PRBS7 up-link is active, the transceiver demodulates purely the SI signal that can be canceled with a proper V_{ctrl1} setting of 0.55–0.7 V (see region [B] in Fig. 22).

TABLE I

PERFORMANCE SUMMARY AND COMPARISON OF PREVIOUSLY PUBLISHED STATE-OF-THE-ART EBD

	Duplexer only					Duplexer with transceiver	
	TMTT'13 [26]	JSSC'13 [27]	ASSCC'15 [28]	TMTT'16 [18]	TMTT'16 [20]	JSSC'16 [10]	**This work [29]**
Center Frequency [GHz]	2	2	2	2.1	30	60	**120**
SI Bandwidth [GHz]	0.5	0.2	0.1	0.229	1	1	**14** *
SI Suppression [dB]	>40	>45	>45	>50	>45	>70	**>30** *
Data Rate [Gbps]	-	-	-	-	-	>5	**6.2**
P_{TX} [mW]	-	-	-	-	-	206	**13.56**
P_{RX} [mW]	-	-	-	-	-	111	**59.41**
$P_{canceler}$ [mW]	-	-	-	-	-	44	**0**
Cancellation Technique	EBD	EBD	EBD	EBD	EBD	Polarization + RF Cancellation	**EBD**
Load	broadband 50 Ω	10-bit array switched resistor	broadband 50 Ω	broadband 50 Ω	Off-chip patch antenna	Off-chip patch antenna	**On-chip bow-tie dipole antenna**
Topology	Fully differential	Single-ended TX Differential RX	Single-ended TX Differential RX	Single-ended RX Differential TX	Single ended	Single ended	**Fully differential**
Technology	90-nm CMOS	40-nm CMOS	28-nm CMOS	0.18-μm SOI CMOS	0.25-μm SiGe BiCMOS	45-nm CMOS	**40-nm CMOS**

* Simulation results

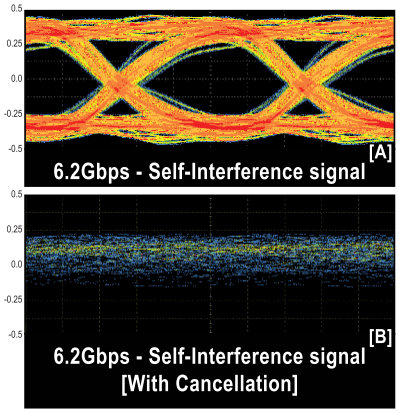

Fig. 20. (a) Measured eye diagrams of the interference signal. (b) Balancing network suppresses that signal if the impedance is tuned correctly.

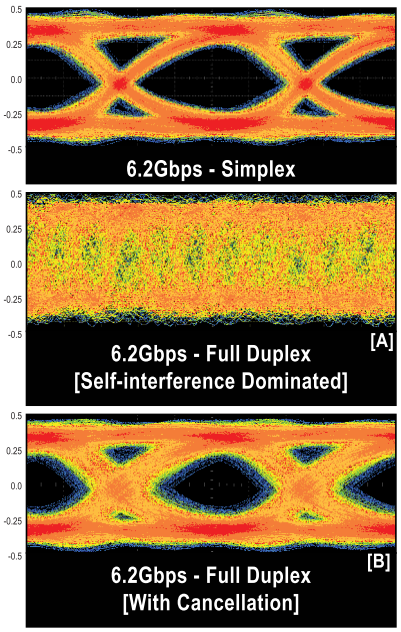

Fig. 21. Measured eye diagrams for (a) simplex communication without interference signal, (b) unbalanced, and (c) balanced IBFD communication.

To improve the duplex performance, one could: 1) design better couplers to improve the effective isolation using chip couplers [3] and 2) reduce the channel loss [25]. This paper shows the capabilities and the limitations when using on-chip antennas.

Fig. 21 demonstrates the isolation performance of the on-chip EBD. With only the PRBS9 down-link active, the eye diagram is shown in Fig. 21(a) resulting in SNR limited demodulation. If the PRBS7 up-link becomes active, the demodulation becomes signal-to-interference-plus-noise ratio (SINR) limited, since the SI signal disturbs the demodulation [see Fig. 21(b)]. After tuning the balancing network to region [B], the SI signal reduces significantly and the eye diagram is presented in Fig. 21(c). Table I summarizes the performance of the proposed IBFD transceiver and compares the results against previously published work. The presented work is the first EBD transceiver with a real on-chip antenna load above 60 GHz. The 14-GHz SI bandwidth is the highest reported to date, resulting in a data rate of 6.2 Gbps.

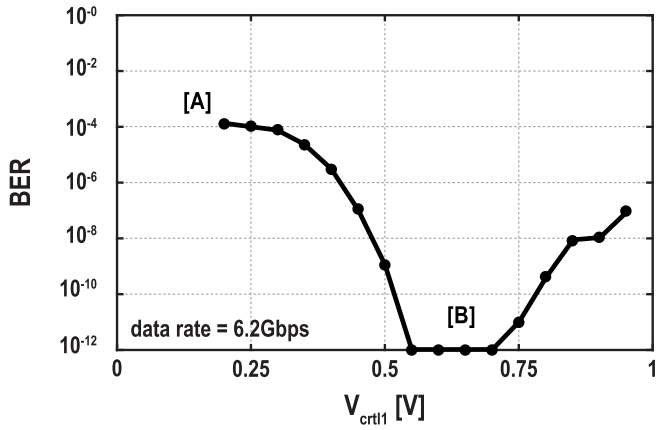

Fig. 22. Measured BER curve for varying V_{ctrl1} while maintaining $V_{\text{ctrl2}} = 0.9$ V.

VI. Conclusion

To achieve bidirectional communication in a PMF link, an orthogonal behavior between up- and down-link has to be realized. This reduces the SI and avoids that both up- and down-link signals become indistinguishable. Typically, time and frequency act as orthogonal signaling dimensions as stated by Goldsmith [6]. In this paper, we investigated the possibility to draw on other orthogonal signaling dimensions: wave direction, wave polarity, and signal polarity. Examples of 120-GHz bidirectional PMF are presented and developed for three different orthogonal cases: 1) an SIW directional coupler on PCB, exploiting orthogonal propagation directions; 2) an IBFD micro-machined OMT design, exploiting orthogonal polarities; and 3) an EBD design in 40-nm CMOS, exploiting signal polarity. First, a 120-GHz SIW directional coupler is implemented and exploits the wave direction orthogonality. The 4-port on-board hybrid coupler achieves measured data rates of, respectively, 6 and 5.5 Gbps in the up- and down-link over a distance of 8 m. Second, a 120-GHz OMT is micro-machined and exploits the wave polarity orthogonality. The micro-machined polarization duplexer has a measured isolation of 45 dB over the entire F-band. For the horizontal and vertical paths, the insertion loss is measured with a 40-cm-long Teflon fiber and varies between -5 and -9 dB. The design of a 120-GHz IBFD PMF transceiver chip with integrated antenna and tunable EBD was proposed and implemented in a 40-nm bulk CMOS technology. Simulation and measurement results were provided. The SI cancellation is performed with a fully differential transformer-based EBD, resulting in a simulated SI suppression of 30 dB over a bandwidth of more than 14 GHz. The insertion loss of the duplexer is less than 11 dB from TX to fiber and less than 12 dB from fiber to RX at a frequency of 120 GHz. The balancing network provides an impedance locking range from 45 to 93 Ω and 38 to 266 fF at 120 GHz with more than 14-GHz bandwidth and 30-dB isolation. For IBFD operation, the maximum measured data rate is 6.2 Gbps using a 120-GHz CPFSK modulation. The dc power consumption is 73 mW in total. The highest level of integration is achieved with the integrated EBD design, where an entire transceiver—including antenna—is implemented on 1.8×1.53 mm^2 silicon. The best results, concerning data rate, are achieved with the OMT design, but this implementation is rather bulky.

Acknowledgment

The authors would like to thank Infineon Technologies AG for their support.

References

[1] N. van Thienen, W. Volkaerts, and P. Reynaert, "A multi-gigabit CPFSK polymer microwave fiber communication link in 40 nm CMOS," *IEEE J. Solid-State Circuits*, vol. 51, no. 8, pp. 1952–1958, Aug. 2016.

[2] P. Reynaert *et al.*, "Polymer microwave fibers: A blend of RF, copper and optical communication," in *Proc. IEEE Eur. Solid-State Circuits Conf. (ESSCIRC)*, Lausanne, Switzerland, Sep. 2016, pp. 15–20.

[3] N. van Thienen, Y. Zhang, M. De Wit, and P. Reynaert, "An 18 Gbps polymer microwave fiber (PMF) communication link in 40 nm CMOS," in *Proc. IEEE Eur. Solid-State Circuits Conf. (ESSCIRC)*, Lausanne, Switzerland, Sep. 2016, pp. 483–486.

[4] S. Fukuda *et al.*, "A 12.5+12.5 Gb/s full-duplex plastic waveguide interconnect," *IEEE J. Solid-State Circuits*, vol. 46, no. 12, pp. 3113–3125, Dec. 2011.

[5] S. Fukuda *et al.*, "A 12.5+12.5 Gb/s full-duplex plastic waveguide interconnect," in *IEEE Int. Solid-State Circuits Conf. (ISSCC) Dig. Tech. Papers*, Feb. 2011, pp. 150–152.

[6] A. Goldsmith, *Wireless Communication*. Cambridge, U.K.: Cambridge Univ. Press, 2005.

[7] Z. Zhang, X. Chai, K. Long, A. V. Vasilakos, and L. Hanzo, "Full duplex techniques for 5G networks: Self-interference cancellation, protocol design, and relay selection," *IEEE Commun. Mag.*, vol. 53, no. 5, pp. 128–137, May 2015.

[8] A. Sabharwal, P. Schniter, D. Guo, D. W. Bliss, S. Rangarajan, and R. Wichman, "In-band full-duplex wireless: Challenges and opportunities," *IEEE J. Sel. Areas Commun.*, vol. 32, no. 9, pp. 1637–1652, Sep. 2014.

[9] A. Arbabian, N. Dolatsha, and N. Saiz, "Fully packaged millimetre-wave dielectric waveguide with multimodal excitation," *Electron. Lett.*, vol. 51, no. 17, pp. 1339–1341, Aug. 2015.

[10] T. Dinc, A. Chakrabarti, and H. Krishnaswamy, "A 60 GHz CMOS full-duplex transceiver and link with polarization-based antenna and RF cancellation," *IEEE J. Solid-State Circuits*, vol. 51, no. 5, pp. 1125–1140, May 2016.

[11] B. van Liempd *et al.*, "RF self-interference cancellation for full-duplex," in *Proc. 9th Int. Conf. Cognit. Radio Oriented Wireless Netw.*, Jun. 2014, pp. 526–531. [Online]. Available: http://eudl.eu/doi/10.4108/icst.crowncom.2014.255756

[12] B. van Liempd, J. Craninckx, R. Singh, P. Reynaert, S. Malotaux, and J. R. Long, "A dual-notch +27dBm TX-power electrical-balance duplexer," in *Proc. IEEE Eur. Solid-State Circuits Conf. (ESSCIRC)*, Sep. 2014, pp. 463–466.

[13] B. Debaillie *et al.*, "In-band full-duplex transceiver technology for 5G mobile networks," in *Proc. IEEE Eur. Solid-State Circuits Conf. (ESSCIRC)*, Sep. 2015, pp. 84–87.

[14] B. van Liempd *et al.*, "A +70 dBm IIP3 single-ended electrical-balance duplexer in 0.18 μm SOI CMOS," in *IEEE Int. Solid-State Circuits Conf. (ISSCC) Dig. Tech. Papers*, Feb. 2015, pp. 32–33.

[15] B. van Liempd, B. Hershberg, B. Debaillie, P. Wambacq, and J. Craninckx, "An electrical-balance duplexer for in-band full-duplex with <-85 dBm in-band distortion at +10 dBm TX-power," in *Proc. Eur. Solid-State Circuits Conf.*, Sep. 2015, pp. 176–179.

[16] B. Hershberg, B. van Liempd, X. Zhang, P. Wambacq, and J. Craninckx, "A dual-frequency 0.7-to-1 GHz balance network for electrical balance duplexers," in *IEEE Int. Solid-State Circuits Conf. (ISSCC) Dig. Tech. Papers*, Feb. 2016, pp. 356–358.

[17] B. van Liempd, B. Hershberg, P. Wambacq, and J. Craninckx, "An integrated tunable electrical-balance filter with stopband tuning range," in *Proc. 11th Eur. Microw. Integr. Circuits Conf.*, Oct. 2016, pp. 1429–1432.

[18] B. van Liempd *et al.*, "A +70-dBm IIP3 electrical-balance duplexer for highly integrated tunable front-ends," *IEEE Trans. Microw. Theory Techn.*, vol. 64, no. 12, pp. 4274–4286, Dec. 2016. [Online]. Available: http://ieeexplore.ieee.org/document/7589000/

[19] C. Lu, M. K. Matters-Kammerer, R. Mahmoudi, and P. G. M. Baltus, "A millimeter-wave tunable transformer-based dual-antenna duplexer with 50 dB isolation," in *Proc. IEEE Custom Integr. Circuits Conf. (CICC)*, Sep. 2014, pp. 1–4.

[20] C. Lu, M. K. Matters-Kammerer, A. Zamanifekri, A. B. Smolders, and P. G. M. Baltus, "A millimeter-wave tunable hybrid-transformer-based circular polarization duplexer with sequentially-rotated antennas," *IEEE Trans. Microw. Theory Techn.*, vol. 64, no. 1, pp. 166–177, Jan. 2016.
[21] A. Bøifot, E. Lier, and T. Schaug-Pettersen, "Simple and broadband orthomode transducer," *IEE Proc. H-Microw., Antennas Propag.*, vol. 137, no. 6, pp. 396–400, Dec. 1990. [Online]. Available: http: http://digital-library.theiet.org/content/journals/10.1049/ip-h-2.1990.0071
[22] G. Pisano *et al.*, "A broadband WR10 turnstile junction orthomode transducer," *IEEE Microw. Wireless Compon. Lett.*, vol. 17, no. 4, pp. 286–288, Apr. 2007.
[23] A. Navarrini and R. Nesti, "Symmetric reverse-coupling waveguide orthomode transducer for the 3-mm band," *IEEE Trans. Microw. Theory Techn.*, vol. 57, no. 1, pp. 80–88, Jan. 2009.
[24] L. Laughlin, M. A. Beach, K. A. Morris, and J. L. Haine, "Electrical balance duplexing for small form factor realization of in-band full duplex," *IEEE Commun. Mag.*, vol. 53, no. 5, pp. 102–110, May 2015.
[25] A. Standaert, M. Rousstia, S. Sinaga, and P. Reynaert, "Analysis and experimental verification of the HE11 mode in hollow PTFE fibers," in *Proc. Asia–Pacific Microw. Conf. (APMC)*, Dec. 2015, pp. 1–3.
[26] S. H. Abdelhalem, P. S. Gudem, and L. E. Larson, "Hybrid transformer-based tunable differential duplexer in a 90-nm CMOS process," *IEEE Trans. Microw. Theory Techn.*, vol. 61, no. 3, pp. 1316–1326, Mar. 2013.
[27] M. Mikhemar, H. Darabi, and A. A. Abidi, "A multiband RF antenna duplexer on CMOS: Design and performance," *IEEE J. Solid-State Circuits*, vol. 48, no. 9, pp. 2067–2077, Sep. 2013.
[28] M. Ramella, I. Fabiano, D. Manstretta, and R. Castello, "A 1.7-2.1 GHz +23 dBm TX power compatible blocker tolerant FDD receiver with integrated duplexer in 28 nm CMOS," in *Proc. Asian Solid-State Circuits Conf. (A-SSCC)*, Nov. 2016, pp. 1–4.
[29] N. van Thienen and P. Reynaert, "A 120 GHz in-band full-duplex PMF transceiver with tunable electrical-balance duplexer in 40 nm CMOS," in *Proc. Eur. Solid-State Circuits Conf.*, Leuven, Belgium, Sep. 2017, pp. 103–106.

Niels Van Thienen (S'12) was born in Turnhout, Belgium, in 1989. He received the M.S. degree in electrical and electronics engineering and the Ph.D. degree in engineering science (electrical engineering) from the University of Leuven, Leuven, Belgium, in 2012 and 2018, respectively.

He is currently a Senior Hardware Engineer with Byteflies, Antwerp, Belgium.

Dr. Van Thienen was a recipient of the 2nd place in the 2016 IEEE SSCS Benelux Chapter chip Design Contest for his work on a polymer waveguide communication link.

Yang Zhang (S'15) received the M.Sc. degree in electromagnetic field and microwave technology from the Harbin Institute of Technology, Harbin, China, in 2013. He is currently pursuing the Ph.D. degree from the University of Leuven, Leuven, Belgium.

His current research interests include millimeter-wave CMOS power amplifier, transmitter, and packaging design.

Patrick Reynaert (SM'11) was born in Wilrijk, Belgium, in 1976. He received the Master of Industrial Sciences in Electronics (ing.) from the Karel de Grote Hogeschool, Antwerpen, Belgium, in 1998, and the Master of Electrical Engineering (ir.) and Ph.D. degrees in engineering science from the University of Leuven (KU Leuven), Leuven, Belgium, in 2001 and 2006, respectively.

From 2006 to 2007, he was a Post-Doctoral Researcher with the Department of Electrical Engineering and Computer Sciences, University of California at Berkeley, Berkeley, CA, USA, with the support of a BAEF Francqui Fellowship. In 2007, he was a Visiting Researcher with Infineon, Villach, Austria. Since 2007, he has been with the Department of Electrical Engineering, KU Leuven, as a Professor. His current research interests include millimeter-wave and tetrahertz CMOS circuit design, high-speed circuits, and RF power amplifiers.

Dr. Reynaert is the Chair of the IEEE SSCS Benelux Chapter. He was a recipient of the 2011 TSMC-Europractice Innovation Award, the ESSCIRC-2011 Best Paper award, and the 2014 2nd Bell Labs Prize. He serves on the Technical Program Committees of several international conferences including ISSCC, ESSCIRC, RFIC, PRIME, and IEDM. He has served as an Associate Editor for the IEEE TRANSACTIONS ON CIRCUITS AND SYSTEMS I, and a Guest Editor for the *Journal of Solid-State Circuits*.